Multimode dynamics in laser diodes with optical feedback

Iestyn Pierce, Paul Rees, and Paul S. Spencer
School of Electronic Engineering and Computer Systems, University of Wales, Bangor, Dean Street, Bangor, Gwynedd LL57 1UT, United Kingdom
(Received 5 November 1999; published 6 April 2000)

The dynamical behavior of semiconductor lasers subject to external optical feedback is analyzed using an approach based on the theory of whole-universe laser modes [R. Lang, M.O. Scully, and W. Lamb, Phys. Rev. A **7**, 1788 (1972)]. The system is modeled as a coupled cavity formed by the laser diode and an external reflector. The leakage of each optical mode out of the cavity is characterized by its mode lifetime. The variation of the cavity mode lifetimes is the dominant mechanism which determines the regime of operation. The method yields the expected range of phenomena observed when a laser diode is subjected to optical feedback, without *a priori* assumptions of the regime of behavior or of the resulting mode wavelengths. For strong optical feedback the imbalance of the lifetimes ensures that a single mode dominates. At other feedback levels the system exhibits chaotic dynamics or stable, multimode operation.

PACS number(s): 42.55.Px, 42.65.Sf

I. INTRODUCTION

External optical feedback into the cavity of a semiconductor laser diode can have a profound effect on its behavior. Depending on the magnitude of the feedback the laser diode can operate in one of several regimes of behavior, as described by Tkach and Chraplyvy [1]. Among these regimes are different classes of the narrow linewidth behavior traditionally associated with laser sources. Apart from such stable operation, feedback can result in fully chaotic dynamics with hugely broadened spectra and an associated reduction in coherence length. This catastrophic descent into chaotic operation has been termed *coherence collapse* by Lenstra [2]. Whether the various effects are deleterious (e.g., instability due to unplanned back reflections from link components in optical fibre communications) or useful (as in the case of single-mode operation in tunable external-cavity lasers) it is important to be able to predict their influence on the behavior of systems that incorporate laser diodes.

Most attempts at the theoretical analysis of laser diode systems subject to external optical feedback have made the assumption of a single longitudinal laser mode. The Lang-Kobayashi model [3] is probably the most widely used single-mode analysis of feedback effects in laser diodes. The Lang-Kobayashi method is based on a perturbation approximation, where the external feedback acts as a perturbation to normal solitary laser operation.

Such single mode analyses are at odds with the majority of the reported experimental results, which were obtained with multimode (Fabry-Perot) laser diodes. In a few cases multimode phenomena have been included in modelling laser diodes with optical feedback by extending the Lang-Kobayashi analysis to multiple modes, either in a rate-equation model [4] or in an iterative scheme [5]. In both the multimode Lang-Kobayashi approach and the iterative scheme the system is assumed to have equally spaced longitudinal modes whose wavelengths are each perturbed slightly by the optical feedback. This requires an *a priori* assumption about the number of longitudinal modes and their wavelengths before any simulations are undertaken.

This paper addresses the effect of optical feedback in a fundamentally different way, where the system is described as a coupled cavity system in a method that draws from the early theory of Lamb, Lang and Scully on the whole-universe mode theory of lasers [6,7]. That theory was originally proposed in order to explain the narrow linewidth of lasers, where laser behavior is modeled accounting for the effect of coupling between the Fox-Li [8] modes of the Fabry-Perot laser cavity and an external cavity that models the effect of power leakage into the universe. The original work concentrated on the limiting case of an infinitely long external cavity (i.e., no back reflection in a finite time). In that case the laser line was shown to be very narrow due to the locking together of the many modes of the universe to a single frequency. In contrast, the analysis presented in this paper is for the case when the frequency locking does not occur due to the finite length of the external cavity, and the resulting output power spectrum shows distinct modes. The time evolution of the mode wavelengths and amplitudes is calculated by self-consistently solving for the wavelengths of the coupled-cavity longitudinal modes and the optical susceptibility. In contrast with the Lang-Kobayashi approach, no initial assumptions about the number of cavity modes or of their wavelengths are required. A coupled cavity approach has previously been applied to two-level laser systems [9] with results that agree well with travelling wave models of similar systems, e.g., Ref. [10].

II. THEORY

The system is modeled as a coupled cavity with a semiconductor gain region coupled with an air-filled external cavity, as illustrated in Fig. 1. The structure is bounded by two semi-infinte regions, with air to the left of z_0 and a region with refractive index η_3 to the right of the external cavity at z_2. The value of η_3 is chosen to yield an identical reflectivity to the proposed external reflector

$$\eta_3(\omega) = \frac{1+\sqrt{R_{\mathrm{ext}}(\omega)}}{1-\sqrt{R_{\mathrm{ext}}(\omega)}}, \tag{1}$$

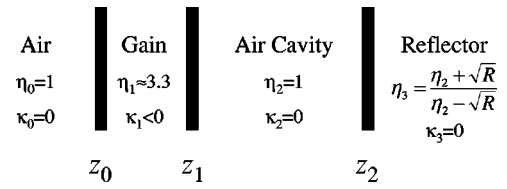

FIG. 1. Laser diode with external reflector as a coupled-cavity system. Refractive index for each section is denoted by η, gain by κ. Negative values of κ indicate a region in gain.

where R_{ext} is the external cavity reflectivity. It is important to note that R_{ext} can be a function of frequency ω as suggested by the expression above for the frequency-dependent refractive index of the reflector region. The boundary between the semiconductor gain region and the external cavity is at z_1. The two outer regions in Fig. 1 are the universe into which optical power leaks in this model.

The inclusion of arbitrary external reflectivities in the model, through Eq. (1), allows the method presented in this paper to be extended to include the effect of frequency-selective feedback. Further extensions to the model could be made to cater for such device structures as distributed-feedback (DFB) lasers or vertical cavity surface-emitting lasers (VCSELs), through suitable modifications to equation (6) in the matrix analysis presented later in this section.

The longitudinal modes of the coupled system are calculated using the method of Ebeling and Coldren, [11], self-consistently with a many-body calculation, [12,13], of the optical susceptibility. The many-body optical susceptibility is included in order to account for the wavelength dependence of the optical gain and refractive index. The many-body calculation includes effects such as bandgap renormalization and Coulomb enhancement which are significant in semiconductor laser materials. It should be noted that a parabolic gain approximation, with an associated linewidth enhancement factor, could be used in place of the many-body calculation. Using such a parabolic gain dispersion curve leads to parabolic features in the resulting output spectrum [14] while the many-body calculation yields spectra that have features more similar to those observed in practical laser diodes, as will be seen in the next section.

The Ebeling-Coldren analysis calculates the wavelength and threshold gain of each of the possible modes of the combination of laser and external cavity. This calculation is undertaken under the assumption of sinusoidally varying electromagnetic fields propagating in both directions in each section of the system depicted in Fig. 1, whose electric field component satisfies the wave equation

$$\frac{d^2E_m}{dz^2}+k_m^2E_m=0. \tag{2}$$

The optical properties of each section are described by the complex propagation constants

$$k_m=\frac{\omega}{c}(\eta_m+i\kappa_m), \tag{3}$$

where η_m is the refractive index of the mth section and κ_m is related to the material gain g_m (in reciprocal meters) by the expression

$$\kappa_m=-\frac{c}{\omega}\frac{g_m}{2}. \tag{4}$$

Each section is assigned a backward-propagating field amplitude A_m and a forward-propagating field amplitude B_m, such that the total field E_m in each section is given by

$$E_m=A_me^{-ik_mz}+B_me^{ik_mz}. \tag{5}$$

By matching the field amplitudes at the interfaces situated at positions z_1, z_2, and z_3, and accounting for the optical gain κ_m in each section, it is possible to write an equation that relates the field amplitudes in the leftmost air section A_0 and B_0 to the amplitudes in the rightmost reflector section A_3 and B_3 via the complex propagation constants.

The only propagation constant that is variable is that of the laser gain section k_1. This may change during the simulations because the refractive index of the gain section η_1 depends on the instantaneous value of the carrier density. The carrier density itself varies with time in accordance with the carrier rate equation, to be described below. At each time step the refractive index η_1 is obtained from the current value of the optical susceptibility.

The resulting equation interlinking the field amplitudes at either end of the system is best written in matrix form

$$\begin{pmatrix}A_3\\B_3\end{pmatrix}=Q(z_2)Q(z_1)Q(z_0)\begin{pmatrix}A_0\\B_0\end{pmatrix}, \tag{6}$$

where each matrix Q is of the form

$$Q(z_j)=\begin{pmatrix}\frac{k_{m+1}+k_m}{2k_{m+1}}e^{i(k_{m+1}-k_m)z_m} & \frac{k_{m+1}-k_m}{2k_{m+1}}e^{i(k_{m+1}+k_m)z_m}\\ \frac{k_{m+1}-k_m}{2k_{m+1}}e^{-i(k_{m+1}+k_m)z_m} & \frac{k_{m+1}+k_m}{2k_{m+1}}e^{-i(k_{m+1}-k_m)z_m}\end{pmatrix}. \tag{7}$$

Since we know that there should be no incoming electromagnetic fields the amplitudes B_0 and A_3 are set to zero. Under this condition, equation (6) can then be solved numerically for the complex propagation constant of the gain section k_1. This is most easily accomplished by writing Eq. (6) in the following form:

$$\begin{pmatrix} 0 \\ B_3 \end{pmatrix} = \mathcal{Q} \begin{pmatrix} A_0 \\ 0 \end{pmatrix}, \quad \text{where } \mathcal{Q} \equiv Q(z_2)Q(z_1)Q(z_0). \tag{8}$$

This equation stipulates the following condition on k_1 the complex propagation constant of the gain section (where A_0 has been set to unity with no loss of generality):

$$\mathcal{Q}_{1,1} = 0 \tag{9}$$

or

$$\begin{aligned} &\frac{e^{ik_3 z_2}}{8k_3k_0k_1}\{(k_3+k_0)e^{-ik_0(z_2-z_1)}[(k_0+k_1)^2 e^{-ik_1 z_1} \\ &\quad -(k_1-k_0)^2 e^{ik_1 z_1}] - 2i(k_3-k_0) \\ &\quad \times (k_0^2-k_1^2)e^{ik_0(z_2-z_1)}\sin(k_1 z_1)\} = 0, \end{aligned} \tag{10}$$

where the propagation constants k_0, k_1, and k_3 are repeated below for clarity:

$$\begin{aligned} k_0 &\equiv k_2 = \frac{\omega}{c}, \\ k_1 &= \frac{\omega}{c}(\eta_1 + i\kappa_1), \\ k_3 &= \frac{\omega}{c}\frac{1+\sqrt{R_{\text{ext}}}}{1-\sqrt{R_{\text{ext}}}}. \end{aligned} \tag{11}$$

The values of k_1 that satisfy Eq. (10) give the frequency ω_{mode} and threshold gain g_{th} of each possible laser mode:

$$\begin{aligned} \omega_{\text{mode}} &= \frac{c}{\eta_1}\text{Re}\{k_1\}, \\ g_{\text{th}} &= -2\,\text{Im}\{k_1\}, \end{aligned} \tag{12}$$

where it is emphasized that η_1 is treated as a constant at any particular time.

The self-consistent calculation thus accounts for the mode-pulling effects neglected in Ref. [11] by including the effect of the carrier-induced change in the gain section refractive index on the instantaneous mode wavelengths. The coupled cavity approach detailed above is valid when the feedback into the laser device is coherent, as is the case for the majority of interesting phenomena. As in the Lang-Kobayashi and iterative methods the coupled cavity analysis also limits the model to dynamics that occur on time scales longer than the cavity round-trip time.

When finding the frequency and threshold gain of each mode it is not necessary to make an initial assumption of the number of modes that will be found: standard numerical methods for the solution of Eq. (10) can find *all* the possible modes within the gain window of the device. This ensures that all the longitudinal modes of the system, both lasing and nonlasing modes, are accounted for correctly.

The mode calculation is carried out alongside a system of rate equations: one for the carrier density N in the gain section

$$\frac{dN}{dt} = \frac{J}{wq} - \frac{J_{\text{spon}}}{wq} - \sum_l v_g g(\omega_l) S_l - \frac{N}{\tau_e} \tag{13}$$

and m equations for the photon densities S in each of the m coupled-cavity modes

$$\frac{dS_l}{dt} = v_g \Gamma g(\omega_l) S_l + \beta \frac{J_{\text{spon}}}{wq} - \frac{S_l}{\tau_l} \tag{14}$$

In this system of rate equations J is the drive current, w is the width of the quantum well gain region, q is the elementary charge, J_{spon} is the equivalent spontaneous emission current, β is the spontaneous emission coupling factor, v_g is the group velocity, Γ is the confinement factor (assumed to be the same for all modes), and τ_e is the carrier lifetime.

The gain terms $g(\omega)$ in the rate equations are also calculated from the optical susceptibility at every time step. The lifetime τ_l is calculated for each mode via the definition

$$\frac{1}{\tau_l} = \frac{1}{\tau_l^{\text{mir}}} + \frac{1}{\tau^{\text{scatt}}}, \tag{15}$$

where the scattering losses τ^{scatt} are the same for each mode, but the mirror lifetimes are variable and calculated from the expression:

$$\tau_l^{\text{mir}} = \frac{(\text{energy stored in system})}{(\text{energy lost per second})}, \tag{16}$$

which yields, for our system, the expression

$$\tau_l^{\text{mir}} = \frac{\int_{z_0}^{z_1}\langle U_1(z)\rangle dz + \int_{z_1}^{z_2}\langle U_2(z)\rangle dz}{2\sqrt{\dfrac{\epsilon_0}{\mu_0}}(\eta_0|A_0|^2 + \eta_3|B_3|^2)}, \tag{17}$$

where the cycle-averaged energy densities $\langle U_1(z)\rangle$ and $\langle U_2(z)\rangle$ are given by

$$\begin{aligned} \langle U_1(z)\rangle &= 2\epsilon_0\eta_1^2\{|A_1|^2 e^{-g_{\text{th}}z} + |B_1|^2 e^{g_{\text{th}}z}\}, \\ \langle U_2(z)\rangle &= 2\epsilon_0\{|A_2|^2 + |B_2|^2\}. \end{aligned} \tag{18}$$

On evaluating the integrals we find the following expression for the mirror lifetimes:

$$\tau_l^{\mathrm{mir}}=\frac{\eta_1^2\{|A_1|^2(1-e^{-g_{\mathrm{th}}z_1})+|B_1|^2(e^{g_{\mathrm{th}}z_1}-1)\}+2\{|A_2|^2+|B_2|^2\}(z_2-z_1)}{2cg_{\mathrm{th}}(\eta_0|A_0|^2+\eta_3|B_3|^2)}. \tag{19}$$

The threshold gain g_{th} for each mode is already known, and the intermediate field amplitudes A_1, A_2, B_1, B_2, and B_3 are found by applying the matrices $Q(z_1)$, $Q(z_2)$, and $Q(z_3)$ in turn. Strictly, these amplitudes have normalized units since the initial condition $A_0=1$ was chosen in solving Eq. (6), but the expression for the mirror lifetime involves only ratios of amplitudes, rendering any normalization immaterial.

In order to isolate the purely deterministic-chaotic behavior, stochastic processes (Langevin noise terms [15] and mode partition noise) are not included in this analysis. It is interesting to compare the model presented in this paper with the Lang-Kobayashi analysis. The Lang-Kobayashi method is based on a perturbation about the solitary laser case; therefore the operating wavelength is assumed to be known in advance, and a correction to that wavelength is calculated by the perturbation analysis. Basing the model on a perturbation analysis limits its applicability to relatively weak feedback, in order to keep the perturbation small. When the Lang-Kobayashi model is extended to multimode operation similar presuppositions are made about the existence and positions of the modes—a center wavelength is chosen and satellite modes, spaced by the reciprocal of the cavity round trip time, are assumed to exist on either side of the center wavelength. Again, corrections to the wavelength of each mode are made by the perturbation analysis. In contrast the method presented here makes no assumptions about the existence or position of the laser modes. The mode positions and threshold gains are calculated from Eq. (10) at each time step. The multimode extension to the Lang-Kobayashi model also typically assigns a single lifetime to all the modes, while each mode calulated from this analysis has its own lifetime, calculated self-consistently with the mode frequency.

The key to the rich variety of possible phenomena predicted by the model presented in this paper is the effect of the variation in mode lifetime calculated above: different modes can have different lifetimes and each mode lifetime can also change with time. When the mode lifetimes change there is a corresponding variation in the field amplitudes in the coupled cavity which can further effect the lifetimes themselves. This feedback mechanism can give rise to chaotic dynamics in conditions when neither of the sections that make up the coupled-cavity system dominates.

III. RESULTS

Numerical simulations were carried out over a range of external cavity reflectivities. Power spectra for the output laser light were calculated by forming a histogram of the instantaneous mode wavelengths over an interval of time. The resulting spectra are therefore ''average spectra,'' displaying the system's behavior over the whole of the histogram time interval. In the results shown in this paper all spectra are averaged over 1 ns—a value that corresponds to the bandwidth of a typical photodetector—with the histogramming process beginning after the initial turn-on transient has decayed.

To verify that the model correctly predicts laser behavior in the absence of optical feedback an initial run was carried out at a very low external reflectivity, $R_{\mathrm{ext}}\equiv -80$ dB. After the decay of the relaxation oscillation transient the mode spectrum portrayed in Fig. 2 was observed. In the absence of appreciable optical feedback the system is seen to exhibit stable behavior, with the mode envelope reflecting the steady-state gain spectrum. (If a parabolic gain dispersion curve had been chosen, the mode envelope would also resemble a parabola.) In this regime all the mode lifetimes are similar in value and the modal gain profile is the dominant effect in determining the amplitude distribution of the modes. The stability of the mode lifetimes yields corresponding stability in the carrier density which reduces the carrier-induced change in the refractive index. The corresponding reduced mode pulling further reinforces the stability of the mode lifetimes. Once the initial transients have died down the system therefore operates in a stable regime—as expected for a solitary laser.

Figure 3 shows the power spectrum of the system when the external feedback level is set at the much higher level of $R_{\mathrm{ext}}\equiv -6$ dB. This corresponds to the case where the external cavity dominates the behavior of the system. Although each mode is narrow, which implies stable operation with little wavelength variation over time, the amplitude distribution between the modes is markedly different to the solitary laser case. In this external cavity regime the mode with the longest lifetime dominates at the expense of the other, shorter lifetime modes, which only exist at very low relative amplitudes. The long-lifetime mode corresponds to a wave-

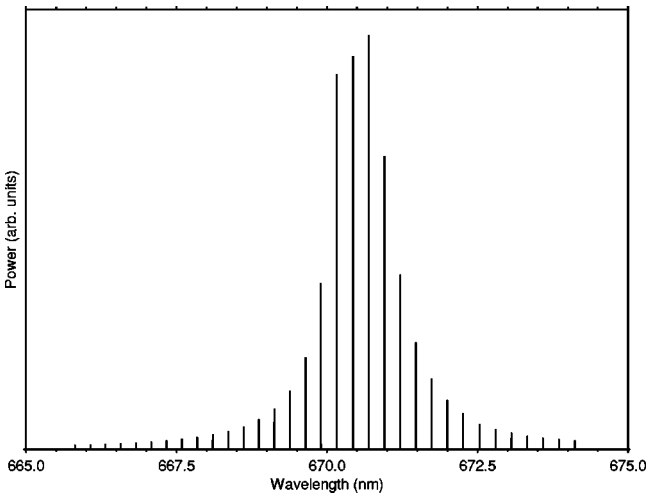

FIG. 2. Power spectrum of solitary laser ($R_{\mathrm{ext}}\equiv -80$ dB), averaged over 1 ns.

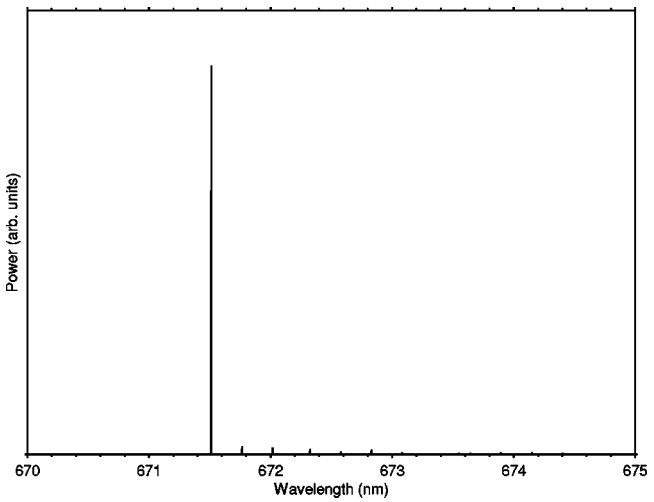

FIG. 3. Spectrum of external cavity laser ($R_{ext} \equiv -6$ dB).

length where the overlap between the notional Fabry-Perot modes of the laser chip and the longitudinal modes of the compound cavity is maximum. This strong single-mode behavior (coupled with tunability through variation of the cavity length) is exactly what makes external cavity laser systems useful in practice. It should be emphasized that the disparity of the mode lifetimes is sufficient to cause single-mode operation. There is no requirement to assume that a single mode should dominate. The wavelength of the dominant mode is also decided without any *a priori* assumptions.

The system behaves very differently when the feedback level is set between the two extremes described above. At feedback levels that correspond to regime IV in Tkach and Chraplyvy's classification scheme the system dynamics are chaotic. Figure 4 shows the output power spectrum for the case $R_{ext} \equiv -28$ dB. The optical modes are barely discernible—the system seems to emit over a broad spectrum. The inset to Fig. 4 illustrates that, in fact, each mode

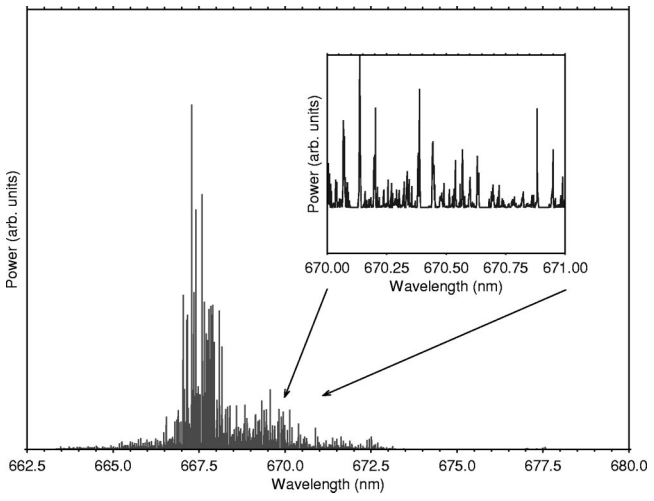

FIG. 4. Spectrum during coherence collapse ($R_{ext} \equiv -28$ dB). Inset shows close-up in range 670–671 nm displaying greatly broadened modes, consistent with the concept of coherence collapse.

has broadened significantly when compared with solitary-laser or external-cavity operation. This is consistent with the concept of coherence collapse, where the temporal coherence length of the laser mode is drastically reduced as a result of the broadening of the modes. This catastrophic mode broadening is a result of the interplay between the fields in the different sections of the coupled cavity, neither of which dominates. Changes in the carrier density cause corresponding changes in the wavelength of the modes and in the mode lifetimes. The changing mode lifetimes cause further changes in the carrier density and, in the absence of the stabilizing influence of a dominant cavity, lead to limit cycles and eventually fully chaotic dynamics. This route to chaos via time-varying mode lifetimes is a complementary approach to the usual time-delayed field term; its strength is that the regimes of behavior of the system are determined purely by the variations of the mode lifetimes.

IV. CONCLUSIONS

The effect of optical feedback on a semiconductor laser diode was studied using a multimode, coupled-cavity approach, reminiscent of the whole-universe mode theory of Lang, Scully, and Lamb. The range of phenomena observed with varying feedback level agree closely with those observed experimentally, falling into a number of regimes. At the two extremes of feedback level—very high feedback and negligible feedback—the model correctly predicts stable behavior in the external cavity and solitary laser regimes. In the former the similarity of the mode lifetimes means that the mode profile is determined by the gain spectrum, while in the latter the nonuniform lifetime distribution leads to the dominance of one external cavity mode. In the coherence collapse regime the model correctly predicts deterministic chaotic dynamics. During coherence collapse the mode lifetimes vary with time, causing corresponding changes in the carrier density that eventually feed back as further changes in the lifetime, leading to instability and chaos. The model differs from the Lang-Kobayashi analysis by calculating the mode wavelengths and lifetimes from considerations of the forward and backward propagating waves in the coupled cavity rather than calculating a perturbation to a presupposed operating wavelength. The model presented here is also valid for higher feedback levels that the Lang-Kobayashi method, correctly predicting stable, single-mode operation in the external cavity operating regime. In all cases the dynamical behavior and the amplitude distribution of the mode spectrum are completely determined by the level of external optical feedback—no *a priori* assumptions are made about the expected regime of operation or about the expected emission wavelengths.

ACKNOWLEDGMENTS

The authors wish to thank Dr. C. H. Henry for his comments on the method presented here. The authors wish to acknowledge the support of the UK Engineering and Physical Sciences Research Council in funding this work under Grant No. GR/L69459.

[1] R. W. Tkach and A. R. Chraplyvy, IEEE J. Lightwave Tech. **LT-4**, 1655 (1986).
[2] D. Lenstra, B. H. Verbeek, and A. J. den Boef, IEEE J. Quantum Electron. **QE-21**, 674 (1985).
[3] R. Lang and K. Kobayashi, IEEE J. Quantum Electron. **QE-16**, 347 (1980).
[4] A. T. Ryan *et al.*, IEEE J. Quantum Electron. **QE-30**, 668 (1994).
[5] P. S. Spencer and K. A. Shore, Quantum Semiclassic. Opt. **9**, 819 (1997).
[6] M. B. Spencer and W. E. Lamb, Phys. Rev. A **5**, 884 (1972).
[7] R. Lang, M. O. Scully, and W. Lamb, Phys. Rev. A **7**, 1788 (1972).
[8] A. G. Fox and T. Li, Bell Syst. Tech. J. **40**, 453 (1961).
[9] S. E. Hodges *et al.*, J. Opt. Soc. Am. B **14**, 180 (1997); **14**, 191 (1997).
[10] M. Homar, J. V. Moloney, and M. San Miguel, IEEE J. Quantum Electron. **QE-32**, 553 (1996).
[11] K. J. Ebeling and L. A. Coldren, J. Appl. Phys. **54**, 2962 (1983).
[12] H. Haug and S. W. Koch, *Quantum Theory of the Optical and Electrical Properties of Semiconductors* (World Scientific, Singapore, 1990).
[13] F. P. Logue *et al.*, Phys. Rev. B **54**, 16 417 (1996).
[14] J. K. White and J. V. Moloney, Phys. Rev. A **59**, 2422 (1999).
[15] K. Petermann, *Laser Diode Modulation and Noise* (Kluwer Academic Publishers, Boston, 1988).